Exciton-Photon Strong-Coupling Regime for a Single Quantum Dot Embedded in a Microcavity

E. Peter,[1,*] P. Senellart,[1] D. Martrou,[1] A. Lemaître,[1] J. Hours,[1] J. M. Gérard,[2] and J. Bloch[1]

[1]*Laboratoire de Photonique et Nanostructures, LPN/CNRS, Route de Nozay, 91460 Marcoussis, France*

[2]*CEA/DRFMC/SP2M, Nanophysics and Semiconductor Laboratory, 17 rue des Martyrs, 38054 Grenoble Cedex, France*

(Received 7 November 2004; published 1 August 2005)

We report on the observation of the strong-coupling regime between the excitonic transition of a single GaAs quantum dot and a discrete optical mode of a microdisk microcavity. Photoluminescence is performed at various temperatures to tune the quantum dot exciton with respect to the optical mode. At resonance, we observe a clear anticrossing behavior, signature of the strong-coupling regime. The vacuum Rabi splitting amounts to 400 μeV and is twice as large as the individual linewidths.

DOI: 10.1103/PhysRevLett.95.067401 PACS numbers: 78.67.Hc, 78.55.Cr, 78.90.+t

Cavity quantum electrodynamics (CQED) has motivated fascinating experiments in atomic physics these past 20 years [1]. When inserting a single atom inside an optical microcavity, two regimes can be reached, depending on the coupling strength between the atomic transition and the optical cavity mode. In the weak coupling regime, the atom spontaneous emission rate is modified as compared to outside the cavity. This phenomenon is referred to as the Purcell effect [2] and has been experimentally observed in the 1980s [3]. In the strong coupling regime (SCR), the light-matter coupling is stronger so that the spontaneous emission becomes reversible. Photons emitted by the atom inside the cavity mode are reabsorbed, reemitted, etc., giving rise to Rabi oscillations. Using high finesse cavities, this regime has been reported in the early 1990s [4]. Recently, the analogous CQED approach has been applied to the discrete states of semiconductor quantum dots (QD). The control of spontaneous emission with QDs inserted in microcavities has been observed [5–10] and applied to the realization of efficient single photon sources [11,12]. As in atomic physics [13], the SCR with an atomiclike QD state is of fundamental interest for CQED experiments [14] but also for new solid-state devices such as single QD lasers [15] or quantum logical gate. Indeed, the discrete QD states could constitute the elementary building block of the solid-state quantum computer (qubits) [15–17] and the cavity mode would mediate the interaction between qubits [18,19].

In this framework, the equivalent of the atomic transitions are the excitonic transitions of the QD. In the SCR with a single QD inserted in an optical microcavity, the system eigenstates are mixed exciton-photon states spectrally separated at resonance by the Rabi splitting Ω. For coherent manipulation of the mixed states, the Rabi splitting has to be much larger than the individual linewidths δ. From this point of view, the ratio Ω/δ is the important figure of merit. Very recently, SCR has been reported with In(Ga)As-based quantum dots inserted in either a micropillar [20] or a photonic band gap [21] microcavity. In both works, the Rabi splitting is of the same order as the linewidths.

In this Letter, we report on the experimental observation of the strong-coupling regime for a single GaAs QD inserted in a microdisk microcavity. The quantum dots under study are formed by thickness fluctuations of a thin GaAs quantum well (QW). As theoretically predicted [22] and checked experimentally [23–25], such QDs have an oscillator strength much larger than InAs self-assembled QDs. These QDs are inserted in microdisks where the electromagnetic field is strongly confined in high quality factor and small effective volume whispering gallery modes (WGM) [26]. Using temperature tuning, we observe the spectral signature of mixed exciton-photon states by photoluminescence measurements. Combining both a large QD oscillator strength and a small cavity mode volume, we obtain a well resolved Rabi doublet with $\Omega/\delta = 2$, promising for future CQED experiments.

Our sample was grown by molecular beam epitaxy on a GaAs substrate. Growth conditions were optimized to obtain large QDs that present large oscillator strength [22]. After the buffer layer, a 10 min annealing at 640 °C was performed under arsenic flow. Then a 1.5 μm layer of $Al_{0.8}Ga_{0.2}As$ was grown at 555 °C and a 71 nm short-period superlattice of 50% mean Al composition was grown at 600 °C. The active material was then deposited: a 50 nm $Al_{0.33}Ga_{0.67}As$ barrier followed by a 13 monolayer GaAs QW, at a growth rate of 1.5 (1.0) Å s^{-1} for the barrier (QW). The top barrier was grown at 590 °C to decrease element III interdiffusion. Finally, the same 71 nm superlattice was grown. A 120 s growth interruption was performed at each QW interface to smooth the growth surface. We used a scanning tunneling microscope (STM) coupled to the growth chamber to study the surface morphology at each interface after the growth interruption on a test sample [Figs. 1(c) and 1(d)]. At the first interface [Fig. 1(c)], the surface presents a large scale roughness as compared to the exciton (X) Bohr radius ($\approx$8 nm). After growth of 13 GaAs monolayers, the surface is atomically smooth with no islands. The monolayer fluctuations in the QW thickness create attractive potentials of the order of 15 meV that localize the center of mass of the X confined in the QW. Analysis of the STM images shows a lateral QD size

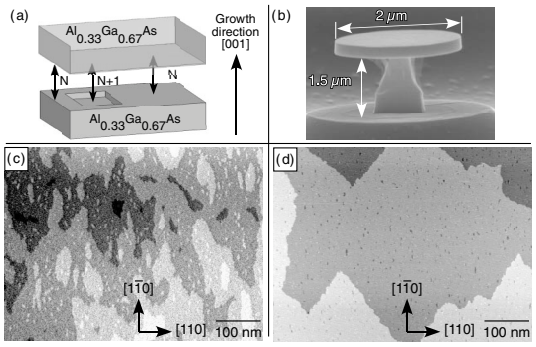

FIG. 1. (a) Schematic of a monolayer fluctuation QD. (b) Scanning electron microscopy side view of a 2 μm diameter microdisk. (c),(d) STM images of both interfaces just after the growth interruption. The color changes correspond to one (Al,Ga)As monolayer change in height.

in the 10 to 100 nm range and an areal QD density around 10 μm^{-2}.

The microdisks [Fig. 1(b)] are obtained by electron beam lithography followed by a two-step chemical etching as described in Ref. [26]. Within such microdisks, WGM can establish: they are vertically confined by the large index contrast between semiconductor and air and guided along the disk circumference by total internal reflection [27].

Photoluminescence measurements are performed at a cryogenic temperature using a cold-finger helium cryostat. The excitation beam is delivered by a continuous wave Ti:sapphire laser (energy 1750 meV) focused with a microscope objective (numerical aperture 0.5) onto a 2 μm diameter excitation spot. The emission, collected at normal incidence by the same objective, is dispersed and detected with a N_2-cooled Si-CCD camera with a 80 μeV spectral resolution.

Figures 2(a) and 2(b) show emission spectra measured on two different microdisks at various temperatures. The spectra in Fig. 2(a) are performed at high excitation power in the density regime where QD lasing occurs in a single WGM and no heating due to the excitation power is observed. The spectra in Fig. 2(b) are measured at low excitation power on a microdisk presenting a well-isolated single QD *X* line as shown in the inset. Both *X* and WGM spectral shifts with temperature are summarized in Fig. 2(c). The QD *X* energy shift with temperature is identical to the bulk GaAs *X* as shown in Fig. 2(c) and in agreement with both theoretical and previously measured values [28]. The redshift of the optical mode with temperature is due to refractive index variation and is identical to the one reported for similar microdisks [9]. The QD *X* line exhibits a stronger spectral shift with temperature than the WGM. These measurements show that temperature scanning allows one both to distinguish *X* versus WGM emission lines and to tune a QD exciton with respect to a lower energy WGM.

Figure 3 presents the spectra on a logarithmic scale obtained on another single microdisk for various tempera-

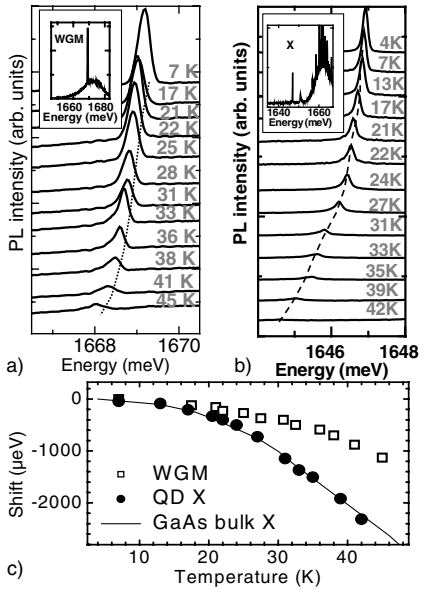

FIG. 2. (a),(b) Photoluminescence spectra (vertically shifted for clarity) measured on two different microdisks between 7 and 45 K. The insets present larger energy scale spectra at the lowest temperature. (c) Spectral shift vs temperature deduced from (a) and (b). Also indicated is the spectral shift of the GaAs bulk exciton.

tures and a low excitation power of 4 μW. The observed photoluminescence lines correspond either to the emission of QD *X* or to the emission of a small background within a WGM. Five optical modes are clearly identified (dotted lines) since they present the same spectral shift with temperature as the one reported in Fig. 2(c). The presence of 5 WGM within a 10 meV spectral window is consistent with the number of modes expected for a 2 μm diameter

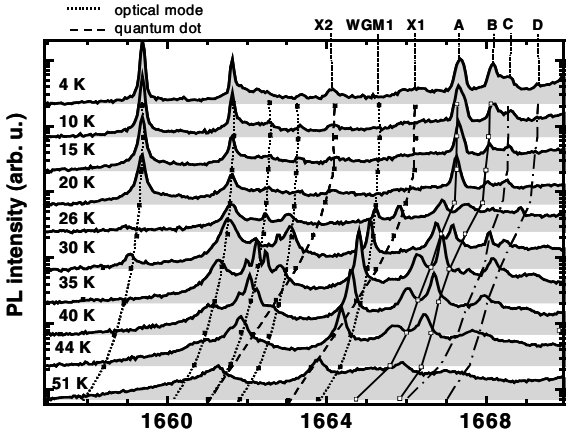

FIG. 3. Photoluminescence spectra (vertically shifted for clarity) on a single microdisk at various temperatures from 4 to 51 K. The dotted (dashed) lines are guides to the eye to follow the emission energy of WGMs (QD *X*s). Solid lines follow spectral shifts different from both a quantum dot and an optical mode spectral shift.

microdisk with 250 nm thickness at this wavelength. Let us now consider the WGM line labeled WGM1 in Fig. 3. It is hardly visible at low temperature and presents a maximum intensity around 35 K. This maximum is explained considering the line labeled $X1$ clearly visible on the high energy side of WGM1 at 26 K. By attributing $X1$ to a QD exciton, we see that 35 K corresponds to the resonance between $X1$ and WGM1. This QD exciton is in the weak coupling regime with the cavity mode. At resonance, because of the Purcell effect, the exciton emits photons preferentially within this mode, so that the emission intensity at the cavity mode energy is enhanced [5,7,10]. Note that the X line labeled $X2$ also gets resonant with two WGM as temperature is increased, resulting in an enhancement of the emission within these optical modes.

Consider now the emission lines A and B in Fig. 3: their spectral shift with temperature differs from the one of both an exciton and an optical mode. A zoom of this region is presented in Fig. 4. When increasing temperature from 4 K up to 26 K, the upper line shifts more than the lower line. This means that the upper line can be assigned to a QD emission, and the lower line to a cavity mode. When increasing temperature, we do not observe a crossing as with $X1$ and WGM1, but an anticrossing, signature of the strong-coupling regime. The eigenstates of the system are not the exciton and photon states anymore, but two exciton-photon mixed states, whose mixing depends on temperature.

Figure 5(a) summarizes the emission energy of the upper and lower lines as a function of temperature. The minimum value of the measured splitting between the two peaks amounts to 400 μeV. Considering $E_C(T)$ and $E_{\mathrm{QD}}(T)$, the energy of the uncoupled cavity mode and QD exciton (as shown in Figs. 2(c) and 5(a)], we can calculate the energy of the two coupled states using [22]

$$E_{\pm}(T) = \frac{E_C(T) + E_{\mathrm{QD}}(T)}{2} \pm \frac{1}{2} \times \sqrt{[E_C(T) - E_{\mathrm{QD}}(T)]^2 + 4g^2},$$

where g is the coupling constant between the exciton and the photon. A very good agreement with the experimental temperature dependence of the lower and upper lines is obtained with $g = 200$ μeV.

These measurements are performed at an excitation power for which the QD X emission is far from saturation at 4 K. When increasing temperature, because of the SCR, the radiative lifetime of the mixed state gets shorter so that the mean excitation number in the system is even smaller. Thus, the system is in a density regime with less than one X in the QD for all temperatures. Therefore, the observed anticrossing is the signature of the vacuum Rabi splitting. The coupling constant of the exciton-photon interaction is thus given by [22] $g = (\frac{1}{4\pi\varepsilon_0\varepsilon_r}\frac{\pi e^2 f}{mV})^{1/2}$ where f is the exciton oscillator strength, V the effective modal volume, m the free electron mass, e the electron charge, and $\varepsilon_0\varepsilon_r$ the dielectric constant. With a 2 μm diameter microdisk, $V = 0.07$ μm^3. From the experimental Rabi splitting, we deduce an exciton oscillator strength of $f = 100$ consistent with reported values [23–25]. This value $f = 100$ is actually a minimum value since there may be a spatial mismatch between the QD and the optical mode antinode which would result in a smaller coupling constant. From Ref. [22], an oscillator strength of 100 corresponds to a

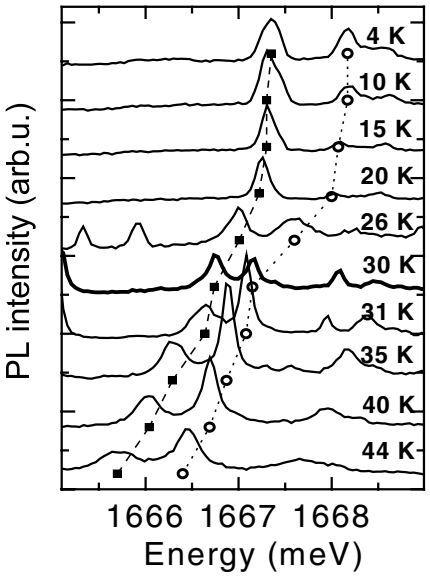

FIG. 4. Photoluminescence spectra on a linear scale (vertically shifted for clarity) for various temperatures between 4 and 44 K. Dashed circles and squares: guide to the eye to follow the energy of the emission peaks for each temperature.

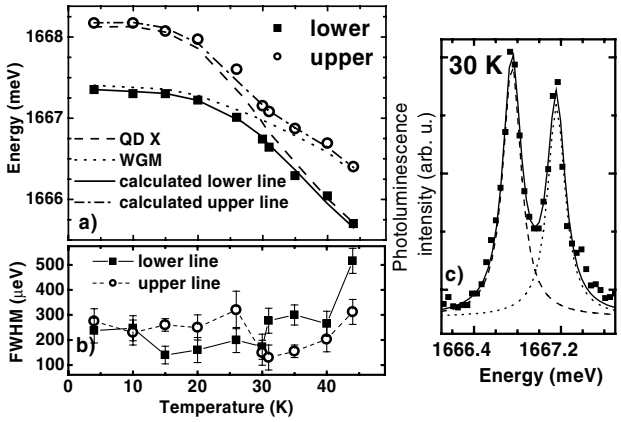

FIG. 5. (a) Symbols: emission energy of the upper and lower lines as a function of temperature. Dashed (dotted) line: spectral shift of a QD X (WGM). Continuous and dash-dotted lines: calculated energy of the two coupled states. (b) Emission linewidth of the lower (squares) and upper (circles) lines as a function of temperature. (c) Squares: Emission spectrum at resonance showing the Rabi doublet. Dashed and dotted lines: Lorentzian fit of each peak. Continuous line: sum of the two Lorentzian lines.

lateral radius of either 6 or 22 nm. According to the STM image, the QD under study most probably presents a radius of around 22 nm. Notice that peaks C and D in Fig. 3 also present an anticrossing, as temperature is changed. So in the same microdisk, some QDs are in the SCR with a WGM, whereas others are not: this is due to variations of the oscillator strength from dot to dot and to their position relative to an antinode of the optical field.

Figure 5(b) summarizes the measured linewidth of the upper and lower lines as a function of temperature. At low temperature (5–25 K), the emission linewidth γ_{WGM} of the photonlike lower line fluctuates between 140 and 250 μeV. These fluctuations are probably due to changes in the residual absorption within the cavity mode that depends on temperature. From these measurements, we can deduce that the quality factor amounts to at least 12 000 for the considered WGM. The emission linewidth γ_X of the excitonlike upper line below resonance amounts to $\approx$280 μeV. This broadening is not radiatively limited but is due to dephasing mechanisms, such as Coulomb interaction with free carriers [29]. Thus, for various sets of data (obtained for the same nominal excitation power but with small variations due to a different excitation condition of the microdisk), the X linewidth fluctuates a little. We report in Fig. 5(b) the averaged linewidth measured at each temperature, and adjust the error bar to these fluctuations. At resonance, because of the half-exciton half-photon nature of the eigenstates, their emission lines present the same linewidth of 180 μeV close to the expected value $(\gamma_{\mathrm{WGM}} + \gamma_X)/2$. Above 40 K, the exciton line (lower line) starts to be thermally broadened.

Another signature of the mixed nature of the eigenstates is found in the measured emission intensities. The X emission is expected to be isotropic, whereas the WGM emits in the microdisk plane so that it is not possible to simultaneously optimize the signal from the X and from the WGM. Indeed, out of resonance, the relative intensity of the upper and lower lines can be slightly modified by changing the collection angle. On the opposite as shown in Fig. 5(c), at resonance, both lines have the same intensity whatever the excitation and collection conditions are.

In 2004, two other groups have demonstrated the SCR for a single quantum dot inserted in an optical microcavity [20,21]. In [21], InAs QDs with small oscillator strength $f = 10$ are inserted in a small effective volume $V = 0.04\ \mu\mathrm{m}^3$ photonic band gap microcavity. In [20], larger oscillator strength $f = 50$ InGaAs natural QD are inserted in a micropillar with a larger effective volume of $0.3\ \mu\mathrm{m}^3$. In both cases, the Rabi splitting is of the same order as the linewidths. In this Letter, we have demonstrated the strong-coupling regime between a large oscillator strength GaAs QD $f = 100$ and a small effective volume microdisk mode $V = 0.07\ \mu\mathrm{m}^3$. Combining large oscillator strength to small effective volume, we have been able to demonstrate a Rabi splitting twice as large as the individual linewidths.

This improvement is a crucial point since it means that when performing coherent control measurements, two Rabi oscillations will take place before decoherence mechanisms occur. Moreover, the microdisk geometry presents several promising advantages: in addition to an easy fabrication process, extremely high quality factors can be achieved associated with small effective volumes. Recently we reported on the fabrication of similar microdisks supported by an aluminum oxide pedestal [30], which allows one to fabricate microdisks as small as desired. By inserting GaAs QD in these microresonators, it would be possible to achieve the SCR with even smaller effective volume. Finally, if several QDs are strongly coupled to the same optical mode, the microdisk geometry can allow one to address selectively each QD, as required for the manipulation of qubits interacting via the electromagnetic field [18].

This work was partly supported by the ''Région Ile de France'' and the ''Conseil Général de l'Essonne.''

*Electronic address: emmanuelle.peter@lpn.cnrs.fr

[1] For a review, see, S. Haroche, Phys. Today **42**, No. 1, 24 (1989).
[2] E. M. Purcell, Phys. Rev. **69**, 37 (1946).
[3] P. Goy *et al.*, Phys. Rev. Lett. **50**, 1903 (1983).
[4] R. J. Thompson *et al.*, Phys. Rev. Lett. **68**, 1132 (1992).
[5] J. M. Gérard *et al.*, Phys. Rev. Lett. **81**, 1110 (1998).
[6] B. Gayral *et al.*, Appl. Phys. Lett. **78**, 2828 (2001).
[7] L. A. Graham *et al.*, Appl. Phys. Lett. **74**, 2408 (1999).
[8] G. Solomon *et al.*, Phys. Rev. Lett. **86**, 3903 (2001).
[9] A. Kiraz *et al.*, Appl. Phys. Lett. **78**, 3932 (2001).
[10] M. Bayer *et al.*, Phys. Rev. Lett. **86**, 3168 (2001).
[11] J.-M. Gérard and B. Gayral, J. Lightwave Technol. **17**, 2089 (1999).
[12] C. Santori *et al.*, Phys. Rev. Lett. **86**, 1502 (2001).
[13] C. J. Hood *et al.*, Phys. Rev. Lett. **80**, 4157 (1998).
[14] J. McKeever *et al.*, Nature (London) **425**, 268 (2003).
[15] For a review, see *Single Quantum Dots*, edited by P. Michler, Topics of Applied Physics (Springer-Verlag, Heidelberg, 2003).
[16] S. N. Molotkov, JETP Lett. **64**, 237 (1996).
[17] F. Troiani *et al.*, Phys. Rev. B **62**, R2263 (2000).
[18] A. Imamoglu *et al.*, Phys. Rev. Lett. **83**, 4204 (1999).
[19] T. Pellizzari *et al.*, Phys. Rev. Lett. **75**, 3788 (1995).
[20] J. P. Reithmaier *et al.*, Nature (London) **432**, 197 (2004).
[21] T. Yoshie *et al.*, Nature (London) **432**, 200 (2004).
[22] L. C. Andreani *et al.*, Phys. Rev. B **60**, 13276 (1999).
[23] T. H. Stievater *et al.*, Appl. Phys. Lett. **80**, 1876 (2002).
[24] J. Hours *et al.*, Phys. Rev. B **71**, 161306(R) (2005).
[25] J. R. Guest *et al.*, Phys. Rev. B **65**, 241310(R) (2002).
[26] B. Gayral *et al.*, Appl. Phys. Lett. **75**, 1908 (1999).
[27] S. L. McCall *et al.*, Appl. Phys. Lett. **60**, 289 (1992).
[28] E. Grilli *et al.*, Phys. Rev. B **45**, 1638 (1992).
[29] C. Kammerer *et al.*, Phys. Rev. B **66**, 041306(R) (2002).
[30] E. Peter *et al.*, Appl. Phys. Lett. **86**, 021103 (2005).